

EXPOSURE OF ERYTHROCYTE SUSPENSIONS SEEDED WITH CONTRAST AGENT MICROBUBBLES IN AN ULTRASOUND STANDING WAVE

S. Khanna⁺, N. N. Amso⁺, S. J. Paynter⁺, and W. T. Coakley[#]

⁺Department of Obstetrics & Gynaecology, University of Wales College of Medicine, Heath Park, Cardiff, CF14 4XN, UK

[#]School of Biosciences, Cardiff University, Main Building, Park Place, PO Box 915, Cardiff CF10 3TL, UK
coakley@cf.ac.uk

Abstract

Human erythrocytes and contrast agent behaviour, both alone and in combination, was studied in standing wave in a single half wavelength chamber driven at its resonance frequency (f_0) of 1.5 MHz. Cells treated alone, formed aggregates in the pressure node plane. However, with contrast agent, first subharmonic ($f_0/2$) and second harmonic ($2f_0$) emissions were detected immediately at pressure amplitude of 0.98 MPa with rapid precession of cells at node plane. Emissions at $3f_0/2$ occurred at 1.47 MPa while white noise and lower order subharmonic emissions coincided with the appearance of visible bubbles at 1.96 MPa. Many precessing erythrocytes were spiculated and were similar to those reported following reversible electroporation. Haemoglobin release was significant under conditions inducing precession with harmonic emissions. It increased discontinuously near the pressure thresholds where more complex frequency emissions were detected. The pattern of haemoglobin release and its association with onset of different acoustic emissions suggests the possibility of defining conditions for controlled sonoporation.

Introduction

Ultrasound-mediated delivery has potential for enhancing and targeting administration of drugs, genes and other therapeutic compounds into and across cells and tissues, including tumours. It has been shown that appropriately applied ultrasound can reversibly permeabilise membranes of viable cells so that exogenous material can enter cells without killing them (1). Much recent work has concentrated on the efficacy of encapsulated contrast microbubbles in causing membrane permeabilisation through cavitation mechanisms both *in vitro* and *in vivo* where the microbubbles themselves may be driven as stable cavities or where their destruction instantly provides cavitation nuclei whose subsequent behaviour will stress cells (2).

The present work explores this possibility by exciting contrast microbubbles and examining the consequences for blood cells close to the pressure node plane of an ultrasound standing wave. It is confirmed that cells at the pressure node are stressed during exposure. The increasing complexity of cavitation emissions detected from the system on increasing pressure amplitude

correlate with cell shape changes and haemoglobin release. The shape changes are similar to those observed when erythrocytes are permeabilised by electroporation.

Methods

Acoustic mini-chamber: A circular standing wave chamber was constructed. Its main components were the transducer, the spacer and the reflector. The transducer had a diameter of 12 mm, a 8 mm rounded back and a half-wavelength pathlength. The transducer surface, attached by a thin layer of epoxy resin to the coupling layer, was electroded over its complete surface while the back electrode was etched (3) to a 8 mm diameter to help create a principal pressure minimum in the central, axial position in the nodal plane (4, 5). The fundamental resonance frequency of the transducer was 1.5 MHz. The thickness of the quartz acoustic reflector was 1.0 mm.

The mini-chamber was designed to produce a high Q resonant system (6). The quartz reflector provided direct microscopic focusing on a node plane.

The basic experimental arrangement for ultrasound generation and amplification has been described in detail elsewhere (5). The transducer was driven by an amplifier, with a sine signal generated by a wave generator. An oscilloscope monitored the voltage across the transducer. A computer, directly connected to the control unit, provided a constant Ultrasound Standing Wave (USW) control. The software 'STAND', developed at Cardiff University, programmed the computer to locate the frequency maximum and then maintain it for a pre-set period.

Optical System and Video Recording : A TV zoom lens and an epi-microscope allowed observation in the direction of the sound propagation (z -) axis (5). A standard PAL CCD camera was fitted with the macroscopic TV zoom lens on one port whereas a Digital High Speed camera (DHSC) capable of capturing images at 500 frames/sec was installed on second port. The active area of the mini chamber was observed either through the binocular eyepieces or through the TV/DHSC port. The sequence of events were videotaped and later converted into a computer files using video capture software for further image processing and analysis. Images captured through

DHSC were automatically stored as .bmp files, which were directly opened by image analysis software.

Acoustic spectrum analysis: A 5 mm diameter piezoceramic disc was mounted in a cylindrical steel holder. The assembly was coupled to the side of circular mini-chamber. The signals from the microphone went to a spectrum analyzer.

Cell and Microbubble source: The experiments were conducted on human blood freshly drawn by venipuncture. Suspensions were made by suspending 2 μ l of blood per millilitre of PBS with 0.1% BSA (PBS/BSA). Suspensions were used within 2 h of preparation. Human albumin microspheres with octofluoropropane (Optison^R) were used as a contrast agent (CA) source for these experiments. A CA concentration of 75 μ l / ml of blood suspension was used (final ratio of Optison microspheres to blood cells was 5:1).

Ultrasound exposure and post-sonication analysis: A peristaltic pump was used to pump the sample into the chamber. The microscope was pre-focused at a selected area of the chamber. The blood cells-CA suspension was gently mixed. The ultrasound and the video recording began immediately after the pump was switched off (batch mode) (5). The cell-CA suspension within the acoustic mini-chamber was exposed to continuous wave 1.56 MHz frequency for pressures varying from 0.98 MPa to 1.96 MPa for different periods ranging from one to ten minutes to study its behaviour in USW.

Estimation of haemoglobin in sonicated samples : Haemoglobin was estimated in samples sonicated for 1 min at different acoustic pressures. After sonication, the samples were collected in eppendorf tubes and centrifuged in a bench centrifuge. The supernatant was used for haemoglobin assay by a plasma haemoglobin assay kit. For comparison, a total haemolysis sample was prepared (positive control) by suspending 2 μ l of blood per ml of distilled water. Haemoglobin was also estimated in a sham sample of cell-CA suspension in PBS/BSA (negative control). The haemoglobin released post-sonication was expressed as a percent of total haemolysis.

Results.

Acoustic emissions and microscopic observations

Cells alone : When cells alone in suspension were exposed to ultrasound (0.98 MPa), they moved to the node plane within a single frame (< 40 ms). Two distinct major aggregates, growing slightly off the chamber centre, were clearly established during the following minute. By the end of 2 min, almost all cells were part of one or other of these clumps. The

aggregated cells were in edge to edge contact and had retained their biconcave shape (Fig. 1). There was no detectable evidence of any shape deformation. When the ultrasound was switched off, the clump of cells disintegrated as it sedimented to the bottom of the acoustic chamber. The phenomenon was consistent for the range of acoustic pressures (0.98 – 1.96 MPa) tested. Drive frequency alone ($f_0 = 1.56$ MHz) was detected on the hydrophone upto a pressure of 1.47 MPa. A second harmonic ($2f_0$) was also detectable when the pressure reached 1.96 MPa. No subharmonic ($f_0/2$) signal was noted within the tested pressure range.

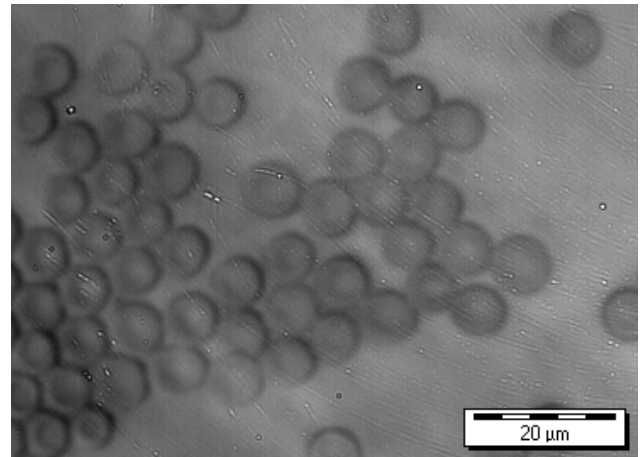


Figure 1. Blood cells aggregation in a USW in the absence of CA (0.98 MPa)

CA alone: When the suspension containing CA was exposed to USW, the bubbles of characteristic contrast agent size, disappeared within a single frame (<40 ms). At pressure amplitude of 0.98 MPa, $f_0/2$ and $2f_0$ were detected. At 1.47 MPa, emission corresponding to $3f_0/2$ was also detected. Finally, white noise appeared at 1.96 MPa. After an exposure of some seconds, a time that decreased as pressure amplitude was increased (0.98-1.96 MPa), large bubbles appeared, formed aggregates and finally clouded the lower surface of quartz glass reflector. This behaviour was noted for all pressures tested. There were no emissions accompanying the appearance of larger bubbles at the lower pressures but the occurrence of subharmonics such as $f_0/3$ at 1.96 MPa suggest that bubbles of a size three times the resonant radius at the drive frequency may have been active at that pressure.

Cell-CA suspension: In contrast to the situation for cells alone, cavitation (as monitored by subharmonic emission) was instantly detected when cell-CA suspension was exposed to USW at a pressure of 0.98 MPa. The blood cells immediately precessed, about the node plane, at its two discrete regions of aggregation as mentioned before for cells alone in suspension (Fig 2). Precessing cells moved in a spiral-like path towards,

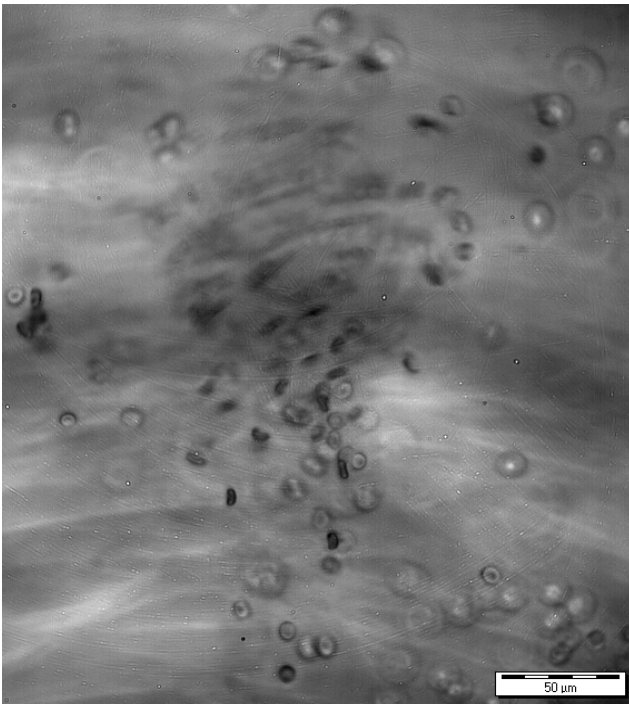


Figure 2. Blood cells in precession in USW in the presence of CA (DHSC; 67 fps; 0.98 MPa)

and then entered, a region where cell movement slowed considerably. The population of precessing cells was refreshed by continuous entry of new cells. The precession phenomenon subsided after 15-20 s coincidentally with the loss of emissions. Cell aggregates then formed in the nodal plane as described above for cell suspensions without CA. Continued exposure to USW resulted in sporadic cavitation and formation of larger bubbles on the lower surface of the quartz glass reflector. Accumulation of large bubbles at this surface finally disturbed the ultrasound field, resulting in settling of blood cells on the base of the chamber.

When cell-CA suspension was sonicated at 1.47 MPa, faster precession at the same discrete regions was observed. Concurrently, sporadic cavitation events caused apparently random rapid cell movements at other points in the node plane. At 1.96 MPa, while the cells remained close to pressure node plane, moved vigorously all over the field without exhibiting a definite pattern. It is note worthy that acoustic emissions were invariably similar to those observed for CA alone at all tested pressures.

Cells during precession appeared to be severely stressed as indicated by an array of shape transformation (Fig 3). Many of the cells that had precessed showed distinct changes in shape and conformation when examined following entry to the quiescent region. The forms included star-like (Fig 3b) and crenated (Fig 3e,f) cells. Indication of protrusion and outgrowth was also suggested on some cells (Fig 3c,d).

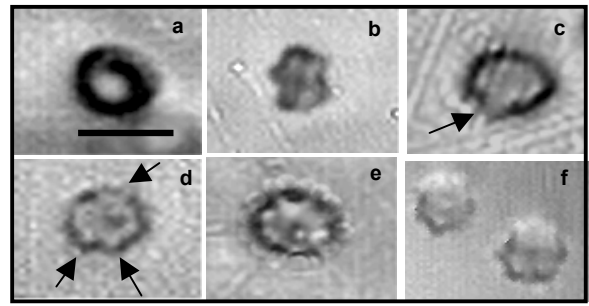


Figure 3. Cells showing varied degree of distortion following precession in USW (0.98 MPa) in presence of CA (DHSC; 67 fps; \blacksquare = 10 μ). (a) Normal, (b) Star shaped, (c & d) Protrusion and outgrowth, (e & f) Crenation

Haemoglobin release: The cells-CA suspension, exposed to USW for 1 min at different acoustic pressure, was tested for haemoglobin release. Haemoglobin content for total haemolysis sample (positive control) was 30 mg/dl (100%). The haemoglobin release in test samples was expressed as a percentage of total haemolysis. Sham Sample (negative control) yielded a release equivalent to 5%.

Haemoglobin release increased discontinuously from 10.25% to 42.60% over pressure amplitude ranging from 0.83 MPa to 1.96 MPa (Fig 4).

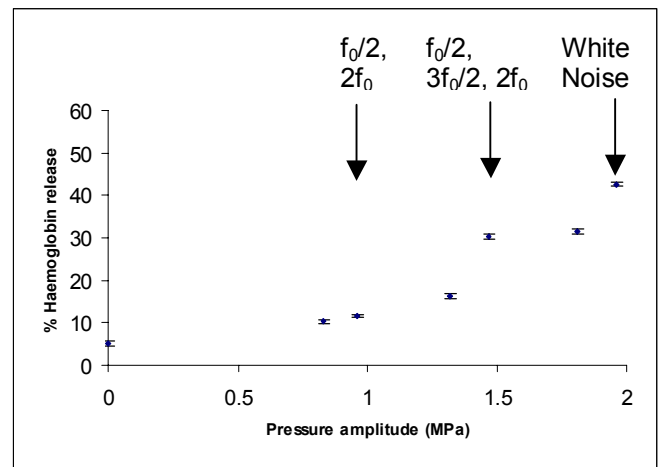


Figure 4. Step changes in haemoglobin release with onset of new emissions in the frequency spectra

A two-fold increase in haemoglobin, as compared to sham, had occurred on the conditions where precession (0.98 MPa) and concurrent subharmonic and second harmonic emissions were observed. At acoustic pressures associated with the first detection of emissions at $3f_0/2$ (1.47 MPa) and white noise (1.96 MPa), a sharp increase in haemoglobin was observed (Fig 4).

Discussion

Significant attention has been directed towards the detection of emissions from microbubbles and contrast

agents. In the present work, onset of second harmonic ($2f_0$) and subharmonic ($f_0/2$) signals were essentially coincident and accompanied by precession of cells. Since neither cell precession nor subharmonic emission was observed in the absence of microbubbles it is reasonable to conclude that microbubbles were responsible for the cell precession. Classical theory on bubble behaviour in a standing wave suggests that bubbles concentrate either at pressure nodes or pressure antinodes depending on whether their fundamental resonance frequencies are below or above the driving frequency. Later it was shown that a spherical bubble whose radius R_0 is just smaller than that, R_{res} , of a bubble resonant at the drive frequency ($0.93 < R_0 < R_{res}$) can execute irregular translational motions about the pressure node plane. Doinikov (7) has recently shown, in an analysis that coupled radial and translational motion that, in principle, any bubble driven below resonance has this property if the pressure amplitude is sufficiently high. Doinikov's analysis was a one-dimensional treatment appropriate for an ideal plane wave. In most real MHz standing wave systems there are pressure differences within and parallel to the node plane (4, 5) so that the force field experienced by bubbles is three-dimensional. Bubbles would in that case be expected to precess about preferred points in the node plane. We argue that the cell precession arises from their entrainment in the hydrodynamic drag of rapidly precessing microbubbles.

The high incidence of spiculated cells in the precessing region was striking. The spiculated forms are clearly different to the parachute forms expected for erythrocytes deformed in a uniform flow field. The persistence of shape change (Fig 3) also argues against passive mechanical deformation by any influence of cavitation-induced flow stress since erythrocyte recovery from mechanical deformation has short relaxation time of the order of several hundred milliseconds. Discocyte-echinocyte changes similar to those reported here were also observed when erythrocytes are exposed to an electroporation procedure (8).

In the present work, haemoglobin release was almost double that measured in unexposed samples at the onset of subharmonic and second harmonic signals (0.98 MPa). A sharp increase in haemoglobin release accompanied both the onset of $3f_0/2$ and the onset of white noise. The stepped pattern of haemoglobin release and the characteristic emissions patterns at the different pressures were confirmed on replicating the experiments thrice. It was concluded that the trend in release was stepwise rather than, for instance, an exponentially growing continuous curve.

In conclusion, USW at 1.5 MHz frequency and pressures ranging from 0.98 MPa to 1.96 MPa induces erythrocyte changes manifested as haemoglobin release and cell crenation. Onset of subharmonic and second

harmonic emission at 0.98 MPa coincides with precession of cells about the pressure node plane. The haemoglobin release increases discontinuously with the increase in pressure amplitude and onset of new emissions. Insights gained from this work may have predictive value in defining conditions for controlled reversible sonoporation.

Acknowledgements:

The authors would like to acknowledge useful discussion with Prof. T. J. Mason and the help extended by Dr. J. Morgan during the initial stage of this study. The work was made possible through capital and equipment grants from the University of Wales College of Medicine.

References

- [1] Guzman HR, Nguyen DX, McNamara AJ, Prausnitz MR. Equilibrium loading of cells with macromolecules by ultrasound: Effects of molecular size and acoustic energy. *J Pharmaceut Sci* 2002; 91: 1693-1701.
- [2] Miller MW, Everbach EC, Cox C, Knapp RR, Brayman AA, Sherman TA. A comparison of the hemolytic potential of Optison and Alunex in whole human blood *in vitro* : Acoustic pressure, ultrasound frequency, donor and passive cavitation detection considerations. *Ultrasound Med Biol* 2001; 27: 709-721.
- [3] Hawkes JJ, Coakley WT. Force field particle filter, combining ultrasound standing waves and laminar flow. *Sensors and actuators B-Chemical* 2001; 75: 213-222.
- [4] Whitworth G, Coakley WT. Particle formation in a stationary ultrasonic field. *J Acoust Soc Am* 1992; 91: 79-85.
- [5] Spengler JF, Jekel M, Christensen KT, Adrian RJ, Hawkes JJ, Coakley WT. Observation of yeast cell movement and aggregation in a small-scale MHz-ultrasonic standing wave field. *Bioseparation* 2001; 6: 329-341.
- [6] Hawkes JJ, Coakley WT, Groschl M, Benes E, Armstrong S, Tasker PJ, Nowotny H. Single half-wavelength ultrasonic particle filter: Predictions of the transfer matrix multilayer resonator model and experimental filtration results. *J Acoust Soc Am* 2002; 111: 1259-1266.
- [7] Doinikov, AA. Translational motion of a spherical bubble in an acoustic standing wave of high intensity. *Phys Fluids* 2002; 14: 1420-1425.
- [8] Chang DC, Reese TS. Changes in membrane structure induced by electroporation as revealed by rapid-freezing electron microscopy. *Biophys J* 1990; 58: 1-12.